Niche separation of wetland birds revealed from airborne laser scanning

Koma, Z.; Grootes, M.W.; Meijer, C.W.; Nattino, F.; Seijmonsbergen, A.C.; Sierdsema, H.; Foppen, R.; Kissling, W.D.

DOI
10.1111/ecog.05371

Publication date
2021

Document Version
Final published version

Published in
Ecography

ECOGRAPHY

Research

Niche separation of wetland birds revealed from airborne laser scanning

Zsófia Koma, Meiert W. Grootes, Christiaan W. Meijer, Francesco Nattino, Arie C. Seijmonsbergen, Henk Sierdsema, Ruud Foppen and W. Daniel Kissling

Z. Koma (https://orcid.org/0000-0002-0003-8258) ✉ (komazsofi@gmail.com), A. C. Seijmonsbergen and W. D. Kissling (https://orcid.org/0000-0002-7274-6755), Univ. of Amsterdam, Inst. for Biodiversity and Ecosystem Dynamics (IBED), Amsterdam, the Netherlands. – M. W. Grootes, C. W. Meijer and F. Nattino, Netherlands eScience Center, Amsterdam, the Netherlands. – H. Sierdsema and R. Foppen, Sovon Dutch Centre for Field Ornithology, Nijmegen, the Netherlands. RF also at: Dept of Animal Ecology and Ecophysiology, Inst. for Water and Wetland Research, Radboud Univ., Nijmegen, the Netherlands.

Ecography
44: 907–918, 2021
doi: 10.1111/ecog.05371

Subject Editor: Nathalie Pettorelli
Editor-in-Chief: Miguel Araújo
Accepted 18 February 2021

Numerous organisms depend on the physical structure of their habitats, but incorporating such information into ecological niche analyses has been limited by the lack of adequate data over broad spatial extents. The increasing availability of high-resolution measurements from country-wide airborne laser scanning (ALS) surveys – a light detection and ranging (LiDAR) technology – now provides unprecedented opportunities for characterizing habitat structure. Here, we use country-wide ALS data in combination with presence–absence observations of birds from a national monitoring scheme in the Netherlands to quantify niche filling, niche overlap and niche separation of three closely-related wetland birds (great reed warbler, Eurasian reed warbler and Savi's warbler). We developed a workflow to derive LiDAR metrics capturing different aspects of vertical and horizontal vegetation structure and used a principal component analysis (PCA), niche equivalency and niche similarity tests to analyse the fine-scale breeding habitat niches of these warbler species in the Netherlands. The widespread Eurasian reed warbler almost completely filled the available wetland habitat space (93%) whereas the two other species showed considerably less niche filling (64% and 74%, respectively). Substantial niche overlap occurred among all species, but each species occupied a distinct part of the habitat space. The great reed warbler mainly occurred in tall and vertically complex wetland vegetation and was absent in areas with large proportions of reedbeds. The Eurasian reed warbler occupied all parts of the wetland habitat space, whereas the Savi's warbler mainly occurred in large homogenous reedbeds with low vegetation height. Our results demonstrate that broad-scale ecological niche analyses can incorporate the fine-scale 3D habitat preference of species with unprecedented detail (e.g. 10 m resolution), and thus go much beyond quantifying the climate niche and 2D habitat information from land cover maps. This is important to identify habitat features and priorities for biodiversity conservation in wetlands and other habitats.

Keywords: *Acrocephalus*, active remote sensing, ecological niche, landscape ecology, *Locustella*, wetland restoration

NORDIC SOCIETY OIKOS

www.ecography.org

Introduction

The quantification of the ecological niche is of fundamental importance for ecology, biogeography and conservation (Grinnell 1917, Hutchinson 1957, Schurr et al. 2012). It provides information on how populations of species can persist (Holt 2009), how multiple species coexist in the same habitat (Chase and Leibold 2003) and how species' respond and adapt to global environmental change (Pearman et al. 2008, Schurr et al. 2012). The rapid development of ecological niche models (Guisan and Thuiller 2005, Soberón and Nakamura 2009, Araújo et al. 2019) and new statistical frameworks for quantitative ecological niche comparisons (Brown and Carnaval 2019) now facilitate studies of ecological niche separation in unprecedented detail, both in geographical (Warren et al. 2008) and environmental space (Broennimann et al. 2012). Such methods allow us to assess whether the ecological niches of two species are equivalent or whether they are more similar than expected by chance given a background environment (Warren et al. 2008, Broennimann et al. 2012, Brown and Carnaval 2019). Various studies have used such methods to test for similarities and differences in ecological niches of closely related species (Warren et al. 2008) or among different areas of occupancy of the same species, for instance in relation to biological invasions (Petitpierre et al. 2012). However, most broad-scale niche studies focus on characterizing the climatic niche whereas niche aspects related to habitat structure have received less attention.

The growing spatial and temporal availability of spaceborne and airborne remote sensing products offers new opportunities for mapping and monitoring vegetation structure with fine resolution across broad spatial extents (Kerr and Ostrovsky 2003, Pettorelli et al. 2016). Specifically, country-wide airborne laser scanning (ALS) provides a method for quantifying fine-scale vegetation structure across broad spatial extents (Lefsky et al. 2002, Vierling et al. 2008, Kissling et al. 2017). ALS is an active remote sensing method using LiDAR (light detection and ranging) technology to capture information on the 3D structure of vegetation (Lefsky et al. 2002). During ALS measurements, the scanner emits a laser pulse which is reflected back from different parts of the vegetation (e.g. leaves, branches and stems) or from the ground. In order to derive ecologically relevant information, the obtained 3D point cloud needs to be further processed, e.g. into metrics which statistically aggregate the 3D point cloud information within raster cells (Davies and Asner 2014, Bakx et al. 2019). LiDAR metrics can then be used to map animal habitats (Lucas et al. 2019, Koma et al. 2020) or to model the geographical distribution of animals such as birds, mammals and invertebrates (Zellweger et al. 2013, 2014, Bakx et al. 2019). Most applications have shown that the distribution and abundance of birds and other taxa are related to the vertical and horizontal heterogeneity of the vegetation as measured by various LiDAR metrics (Davies and Asner 2014). While several studies have used LiDAR metrics in species distribution models (SDMs) (reviewed by Bakx et al. 2019), their application in studies of niche separation in habitat space (i.e. in environmental rather than geographic space) are rarely carried out (Brown and Carnaval 2019).

LiDAR technology has been predominantly used for quantifying the effect of vegetation structure on animal habitat and space use in forests (Hill et al. 2014). However, recent studies have shown that ALS has also the potential to be used in non-forested habitats such as wetlands, e.g. for quantifying vegetation height (Hladik and Alber 2012, Luo et al. 2015, Nie et al. 2018), for mapping the density and biomass of reed beds (Corti Meneses et al. 2017, Luo et al. 2017), or for classifying wetland-related habitat types (Koma et al. 2020). This is remarkable because wetland habitats such as marshes, reedbeds, swamps or peatlands predominantly consist of low vegetation which limits the detection of vegetation structure with LiDAR. One reason is that subsequent laser returns from low vegetation (or dense forest canopies) may be too short to be detected so that only one laser hit is recorded by the sensor (Hopkinson et al. 2005, Hladik and Alber 2012). Nevertheless, low-stature habitats still vary substantially in vegetation structure (e.g. reed height and density) and horizontal structure at the landscape scale (e.g. patchiness and edges) which strongly determines the habitat niche of animals inhabiting wetlands (Gilbert and Smith 2012). For instance, local field studies of reed warblers (songbirds breeding in reedbeds) have shown that their habitat niches are separated by vegetation height and distance from the water (Graveland 1998, Leisler and Schulze-Hagen 2011). Field observations further show that the availability of insects depends on the density of the undergrowth (van der Hut 1985) which shapes the feeding strategies of these species (Leisler and Schulze-Hagen 2011). Other studies have shown that the horizontal distribution of vegetation structure and differences in wetland plant communities (e.g. the homogeneity and extent of reedbeds or the amount and patchiness of bushes) are important components for characterizing the habitat niches of these species at the home range scale (van der Hut 1985, Graveland 1998, Gilbert and Smith 2012). However, most field observations are restricted to local study areas, and it remains unclear how general these animal–habitat relationships are.

Here, we use country-wide ALS data from the Netherlands to test whether the breeding habitat niches of three closely-related wetland birds can be separated in environmental (i.e. vegetation structural) space. We focus on the great reed warbler *Acrocephalus arundinaceus*, the Eurasian reed warbler *Acrocephalus scirpaceus* and the Savi's warbler *Locustella luscinioides* and derive high resolution (10 m) LiDAR metrics to test for niche overlap using niche similarity and niche equivalency tests (Warren et al. 2008, Di Cola et al. 2017). The general breeding habitat niche of these three warblers is highly overlapping (i.e. all species are breeding in reedbeds), but various field studies suggest that they separate their niches at a finer scale along different gradients of vegetation structure (van der Hut 1985, Graveland 1998, Leisler and Schulze-Hagen 2011). Using high quality and detailed bird territory mapping data from a comprehensive national monitoring scheme we test 1)

to what extent niche filling of habitat space as derived from LiDAR metrics differs among the three warblers (with the Eurasian reed warbler being the most widespread and probably least specialized species), and 2) how the use of vertical and horizontal vegetation structure (e.g. height, density of low vegetation, proportion and patchiness of reed) differs among the warbler species (with the great reed warbler potentially preferring tall water reed and the Savi's warbler relatively large and homogenous patches of reed vegetation). Country-wide ALS data thereby allow us to separate the fine-scale breeding habitat niches of wetland birds using a standardized protocol across broad spatial extents. This goes much beyond the coarse habitat information typically provided by other remote sensing products such as land cover maps.

Material and methods

We developed an open-source workflow to process and analyse the bird observation and ALS data (Fig. 1). This included three main processing steps: 1) processing of bird observation data, 2) processing of LiDAR data and 3) statistical analysis of the results. For processing the LiDAR point cloud data at the national scale, we used the recently developed open-source Python toolkit 'Laserchicken' (Meijer et al. 2020) within the associated framework for research applications ('Laserfarm', <https://github.com/eEcoLiDAR/Laserfarm>). The developed workflow (Fig. 1) is freely available as R scripts via GitHub (<https://github.com/eEcoLiDAR/Niche_separation_wetland_ALS>).

Processing of bird observation data

The breeding bird observations were collected by Sovon (Dutch Centre for Field Ornithology, <www.sovon.nl/en>) which coordinates the monitoring of wild bird populations in the Netherlands. We used the bird observations from 2014 to 2018 collected by the breeding bird monitoring program (BMP) which encompasses areal surveys of territorial behaviour during the breeding season (territory mapping). The time span of the bird observations matched the LiDAR data acquisition time and provided presence–absence information within survey plots across the Netherlands using a standardized field sampling protocol with a similar observation effort across species (Vergeer et al. 2016). Each year between March and July all survey plots (ranging from 10 to 500 ha in size) were visited 5–10 times in the early morning by an experienced ornithologist. During the field visits the spatial location of all birds with territorial and nest indicative behaviour (e.g. song, alarm, nest) were mapped. The sampling scheme thus provides high-resolution presence data (i.e. exact spatial locations of observed individuals during the breeding season)

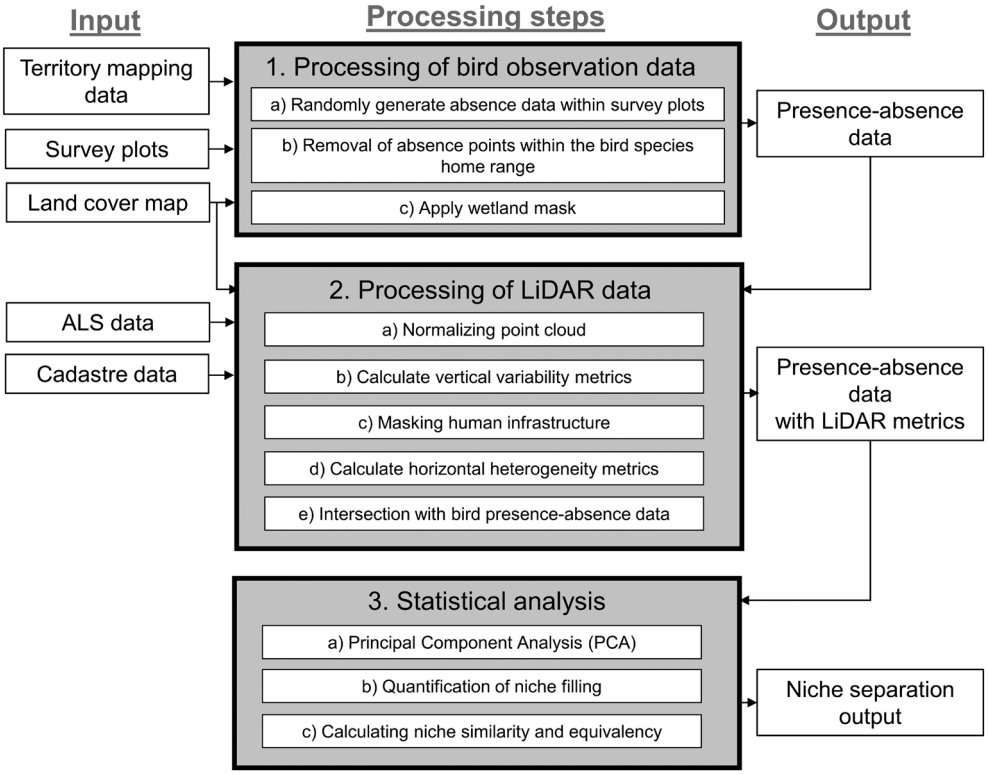

Figure 1. Workflow for analysing habitat niches of wetland birds using field observations (presence–absence data derived from territory mapping within survey plots) from a national monitoring scheme and country-wide airborne laser scanning (ALS) data based on light detection and ranging (LiDAR). The workflow contains three main processing steps (grey boxes). Input datasets are located on the left side and output on the right side (in white boxes).

as well as absence information (i.e. those areas within survey plots in which a species has not been observed given a standardized sampling effort).

We selected three wetland bird species which prefer reedbeds as their breeding habitat: the great reed warbler *Acrocephalus arundinaceus*, the Eurasian reed warbler *Acrocephalus scirpaceus* and the Savi's warbler *Locustella luscinioides*. All three species are closely related and belong to the Old World warblers. We used a 200 m radius around each bird observation point to characterize the habitat use of each bird. This corresponds to the estimated activity range of these species based on observational data from Sovon and the literature (van der Hut 1985). To select absence points, we randomly placed points in the survey plots (Fig. 1, substep 1a) and only included those which 1) were outside a 200 m radius around presence points (Fig. 1, substep 1b), and 2) spatially coincided with wetland land cover types (Fig. 1, substep 1c; Supporting information). This provided absence points within areas that had been intensively surveyed but without recording the species (i.e. wetland land cover types within sampled survey plots, but sufficiently away from recorded presences). To select wetland land cover types, we constructed a wetland mask using the Dutch land cover map (Landelijk Grondgebruik Nederland, LGN2018) which is based on high-resolution satellite imagery and aerial photographs at 5 m resolution. The wetland mask included five wetland-related LGN2018 land cover classes: open water, salt marsh, shrub vegetation in wetlands, reedbeds and forest in wetlands. A total of 453, 83 613 and 9005 presence records were included for the great reed warbler, Eurasian reed warbler and Savi's warbler, respectively. We initially generated 150 000 random absence points within the survey plots and finally used a total of 6307 absence points after applying the wetland mask and the activity range around presence points. We used both presence and absence records for characterizing the background environment (i.e. wetland habitat space). The total covered area in this study was 3600 km^2.

Processing of LiDAR data

The LiDAR data were acquired during the third Dutch national ALS flight campaign (AHN3, Actueel Hoogtebestand Nederland) between 2014 and 2019 during the spring, autumn and winter months. The AHN3 dataset is openly accessible, captures multiple returns and has an average point density of 8 pt m^{-2} (<https://ahn.arcgisonline.nl/ahnviewer/>). The raw point cloud has been pre-processed by 'Rijkswaterstraat' (the executive agency of the Dutch Ministry of Infrastructure and Water Management) and comes with a classification of ground, building, water and non-ground points. Our study covers the whole Netherlands, except for the province of Groningen, because those point clouds were not yet released when conducting the analyses. The processing of the AHN3 data for the purpose of this study consisted of five substeps (Fig. 1, step 2 a–e).

First, the point cloud data were normalized by subtracting the terrain height from the height of each point. The digital terrain model was defined by using the minimum height of points in each 1 × 1 m cell (Fig. 1, substep 2a).

Second, points associated with the ground, water or buildings were dropped, resulting in a point cloud that can be attributed to vegetation. With these points we calculated various LiDAR metrics capturing vertical vegetation structure within 10 m resolution grid cells (Fig. 1, substep 2b). We selected metrics including height, foliage height diversity and vegetation density within specific strata (Table 1). These are commonly used in LiDAR-based habitat studies of birds (Bakx et al. 2019) and capture complementary measurements of vertical vegetation structure that are relevant for the selected reed warbler species (Table 1).

Third, we applied various data filters to ensure that the grid cells including human infrastructures were removed (Fig. 1, substep 2c). We excluded grid cells overlapping with cities and rail tracks based on information from the LGN2018 data. Because power lines are not included in LGN2018, we filtered them directly based on the TOP10NL cadastre data (<https://zakelijk.kadaster.nl/-/top10nl>) using a 20 m buffer around the polylines and intersecting these with the 10 m LiDAR metrics dataset.

Fourth, we calculated second-order LiDAR metrics that capture the horizontal heterogeneity of vegetation within the 200 m radius around bird observations (Fig. 1, substep 2d). This was done with a moving window approach based on the 95th percentile of vegetation height in 10 m grid cells (VV_p95, Table 1) and a radius of 200 m around a focal grid cell. These LiDAR metrics were either based on the standard deviation (SD) of VV_p95 or on the proportion and patchiness of reed and helophyt vegetation (Table 1). Reed and helophyt vegetation was defined by using a VV_p95 threshold (> 1 m and < 3 m) to differentiate reedbeds from other vegetation such as bushes and trees (> 3 m) because the height of reed *Phragmites australis* and other helophyts (e.g. *Typha angustifolia*) in our study area typically lies between 1 and 3 m. This threshold was then used to derive the SD of reed vegetation (HH_reedveg_sd) and to capture the proportion and the number of patches of reed and helophyt vegetation within a 200 m radius (Table 1). Patches were defined as spatially connected grid cells (using a queens neighbourhood, i.e. the eight adjacent grid cells). We also included one horizontal variability metric of total vegetation (HH_sd, Table 1).

Fifth, we intersected the LiDAR metrics with the bird observation data, i.e. with both the presence and absence points (Fig. 1, substep 2e). We excluded observation points where the 95th percentiles of normalized height was above 30 m. This step was necessary to exclude any remaining human infrastructures (e.g. wind turbines) that could not be filtered out using the cadastre data.

Statistical analyses

The statistical analysis included four parts (Fig. 1, substeps 3a–c). First, we performed a principal component analysis (PCA) (Fig. 1, substep 3a) to reduce the dimensionality of the nine LiDAR metrics and because subsequent niche similarity

Table 1. LiDAR metrics for studying ecological niche overlap among reed warblers. Metrics capturing vertical vegetation structure were directly calculated from the LiDAR point cloud at 10 m grid cell resolution whereas horizontal heterogeneity metrics were calculated using 10 m resolution grid cells of vegetation height values (VV_p95) around a 200 m radius of each focal cells. SD = standard deviation; z = height value of LiDAR point.

Metric name (abbreviation)	Metric calculation	Ecological relevance
Vertical vegetation structure		
Vegetation height (VV_p95)	95th percentile of normalized z within 10 m grid cell	Vegetation height of tallest plants (e.g. trees, shrubs, reed)
Foliage height diversity (VV_FHD)	Shannon entropy of normalized z within 10 m grid cell derived from height layers with 0.5 m thickness	Structural complexity of vertical biomass distribution and layering of vegetation
Vegetation density of 0–1 m layer (VD_0_1)	Ratio of number of points < 1 m relative to number of total vegetation points within 10 m grid cell	Density of vegetation in lowest understory layer
Vegetation density of 1–2 m layer (VD_1_2)	Ratio of number of points between 1 and 2 m relative to total number of vegetation points within 10 m grid cell	Density of vegetation 1–2 m above ground
Vegetation density of 2–3 m layer (VD_2_3)	Ratio of number of points between 2 and 3 m relative to total number of vegetation points within 10 m grid cell	Density of vegetation 2–3 m above ground
Horizontal structure of vegetation		
Horizontal variability of total vegetation height (HH_sd)	SD (within 200 m radius) of 95th percentile of normalized z (VV_p95 values of 10 m resolution grid cells)	Heterogeneity of total vegetation height within the home range scale of reed warblers
Horizontal variability of height of reed vegetation and other helophyts (HH_reedveg_sd)	SD (within 200 m radius) of 95th percentile of normalized z (VV_p95), including only those 10 m grid cells that have z > 1 m and z < 3 m	Heterogeneity of reed and helophyt vegetation (with 1–3 m canopy height) within the home range scale of reed warblers
Proportion of reed vegetation and other helophyts (HH_reedveg_prop)	Proportion of 10 m grid cells with z > 1 m AND z < 3 m within 200 m radius, based on 95th percentile of normalized z (VV_p95)	Amount of reed and helophyt vegetation within the home range scale of reed warblers
Patchiness of reed vegetation and other helophyts (HH_reedveg_patch)	Number of patches of reed and helophyt vegetation within 200 m radius (based on 95th percentile of normalized z, including only cells with z > 1 m and z < 3 m)	Homogeneity and coherence of the reed and helophyt vegetation within the home range scale of reed warblers

and equivalency tests are only available for two dimensions. The PCA was done with the presence and absence points of all three bird species (n = 99 404). We assessed the ecological relevance and meaning of the PCA axes by analysing the factor loadings with Pearson's correlation coefficients (r) between the LiDAR metrics and the PCA axes.

Second, we analysed niche filling (Fig. 1, substep 3b) by quantifying the extent to which the available wetland habitat space is occupied by the three species. We calibrated the PCA on the entire environmental (wetland habitat) space (compare PCA-env in Broennimann et al. 2012) using a kernel density function for smoothing the density of presence records within the wetland habitat space (i.e. using all 10 m grid cells intersected with presence and absence records within wetland-related land cover types). The application of a kernel smoother to standardize species densities within the two-dimensional PCA makes moving from a geographical space to a multivariate environmental space independent of both sampling effort and resolution in environmental space (Broennimann et al. 2012). The environmental space (here captured by the first two PCA axes) was divided into a grid of 500 × 500 cells, including all parts with low and high density of presence records. We additionally tested 100 × 100 and 1000 × 1000 grid cell sizes for the multivariate environmental space (Supporting information). Niche filling was then quantified for each species as the percentage of occupied niche space relative to the total available background (i.e. wetland habitat space along the two PCA axes). Niche filling was calculated for both the total occupied area (i.e. no percentile threshold applied for the kernel density) and for high species densities only (i.e. 50th percentile of kernel density).

Third, for calculating niche overlap among pairs of species (Fig. 1, substep 3c), we used the Schoener's D statistic (Warren et al. 2008) which varies from 0 (no overlap) to 1 (complete overlap). This quantifies the amount of niche overlap by computing the absolute differences in densities of occurrences between two species for every grid cell in environmental space. Two tests can then be carried out to assess the statistical significance of the niche overlap with a randomization procedure (Warren et al. 2008, Di Cola et al. 2017, Brown and Carnaval 2019). First, the niche equivalency test assesses whether the niches of two species are identical or not. The randomisation places the occurrences of both species randomly across the density grids of both species in environmental space. If the observed niche overlap value is significantly lower than the frequency distribution of randomized D values, the habitat niches of the two species are different, i.e. they are not equivalent. Second, the niche similarity test assesses whether the overlap between the observed niches of two species significantly differs from the frequency distribution of overlaps

when the habitat niche of one species is randomly allocated in the environmental background by shifting the centroid of its occurrence density grid (Di Cola et al. 2017). This is done 1000 times and the similarity between each simulated density plot and the observed density plot is then calculated (Supporting information). If the observed D value is significantly greater than the frequency distribution of the random D values, it indicates that the species' niches are more similar than expected by chance given the available environmental space (here wetland habitat structure). If the niche similarity test is not significant, it indicates that the niches are not similar, i.e. they do not substantially overlap. For both statistical tests, we used 1000 randomisations and assessed a difference to be statistically significant when the observed value of D fell outside the 95% of the simulated values (i.e. equivalent to $p < 0.05$ for a one sided test).

Results

The PCA reduced covariation among the nine LiDAR metrics into two main dimensions (PCA 1 and PCA 2; Fig. 2d). PCA 1 explained 37% and PCA 2 24% of the variance, with any other axis only contributing ≤ 10%. PCA 1 was mainly characterized by LiDAR metrics capturing the vertical structure of vegetation around bird observation points (10 m resolution), specifically foliage height diversity (VV_FHD), vegetation density between 0 and 1 meters (VD_0_1) and vegetation height (VV_p95) (Fig. 2d, variable loadings in Supporting information). Hence, large and positive values of PCA 1 reflected tall and vertically complex wetland vegetation with a low density of herbaceous vegetation < 1 m. PCA 2 mainly reflected horizontal vegetation structure within a radius of 200 m around the bird observation points (Fig. 2d), i.e. a high proportion and large areal extent of reedbeds (HV_reedveg_prop) with little fragmentation and few patches (HV_reedveg_patch) (variable loadings in Supporting information). Some LiDAR metrics did not load clearly on only one PCA axis, e.g. vegetation density (VD_1_2) and two of the horizontal heterogeneity metrics (HV_reedveg_sd and HV_reedveg_patch, factor loadings in the Supporting information).

Niche filling (Fig. 2e–g) was greatest for the Eurasian reed warbler, with about 94% of the available background environment (wetland habitat space) being occupied by this species (Fig. 2f). The other two species (great reed warbler and Savi's warbler) only filled 64% and 76%, respectively (Fig. 2e, g). Restricting the kernel density estimation to a 50% percentile threshold showed that the great reed warbler had the most restricted density of occurrences in this wetland habitat space (5%), followed by the Savi's warbler (14%) and the Eurasian reed warbler (20%) (Fig. 2e–g).

Besides niche filling, the three bird species also differed in their occurrence densities within the available wetland habitat space (Fig. 2e–g). The great reed warbler had the highest occurrence density in tall and vertically complex vegetation (PCA 1 axis in Fig. 2d), indicating that it is present in reedbeds with tall reeds and some bushes and trees (Fig. 3). In contrast, the Eurasian reed warbler was less specialized, and often occurred in linear strips of reed vegetation along ditches (Fig. 3c), a type of reed habitat that is widespread in the Netherlands. The Savi's warbler occurred in large homogenous reedbeds or other low-stature wetland vegetation interspersed with few bushes or small trees (Fig. 3d). These differences in breeding habitat among the three species were reflected in the occurrence densities of the PCA in which the Eurasian reed warbler showed a wide distribution along both PCA 1 and PCA 2 (Fig. 2f), whereas the Savi's warbler had the highest occurrence densities in large homogenous reed vegetation (PCA 2) with low vegetation height (PCA 1) (Fig. 2g). The great reed warbler was absent in areas with high reedbed proportions (PCA 2 capturing HV_reedveg_prop, Fig. 2e), probably reflecting territories with a large amount of water in the surroundings (no LiDAR vegetation points) since they occur close to the water edges (Fig. 3a–b).

Each species had a distinct occurrence density within the two-dimensional habitat space (Fig. 4). While there was substantial niche overlap among all species (Schoener's D: 0.46–0.61, Table 2), the niche equivalency tests revealed that the observed niche overlaps were substantially smaller than expected by chance, indicating niche separation among all three warbler species (Table 2, Fig. 4).

The niche similarity tests further revealed interesting differences among species pairs (Table 2). The great reed warbler and the reed warbler were the only species for which niche overlap was significantly more similar than expected from random shifts of both occurrence density grids into the background environment (Table 2). This suggested that both species can in principle occupy similar habitat structures. The comparison of Savi's warbler and the Eurasian reed warbler showed no significant difference in the niche similarity test when the Savi's warbler occurrence density grid was shifted, but a significant difference when that of the Eurasian reed warbler was shifted (Table 2). This indicated that the Savi's warbler did not occupy specific habitat structures that the Eurasian reed warbler used, but that the Eurasian reed warbler could occupy habitat structures used by the Savi's warbler. Finally, the comparison of the great reed warbler and the Savi's warbler showed no significant differences in the niche similarity tests (Table 2). This indicated that the two species occupied distinct breeding habitats.

Discussion

Using detailed presence–absence data of birds from a national monitoring scheme together with high resolution LiDAR metrics derived from country-wide ALS data we show that the breeding habitat niches of three closely related reed warbler species can be clearly separated along two major axes of wetland vegetation structure. While all three species show considerable niche overlap, they also differ in their occurrence densities within the wetland habitat space, especially in relation to specific aspects of vertical vegetation structure (e.g. reed height, foliage height diversity and

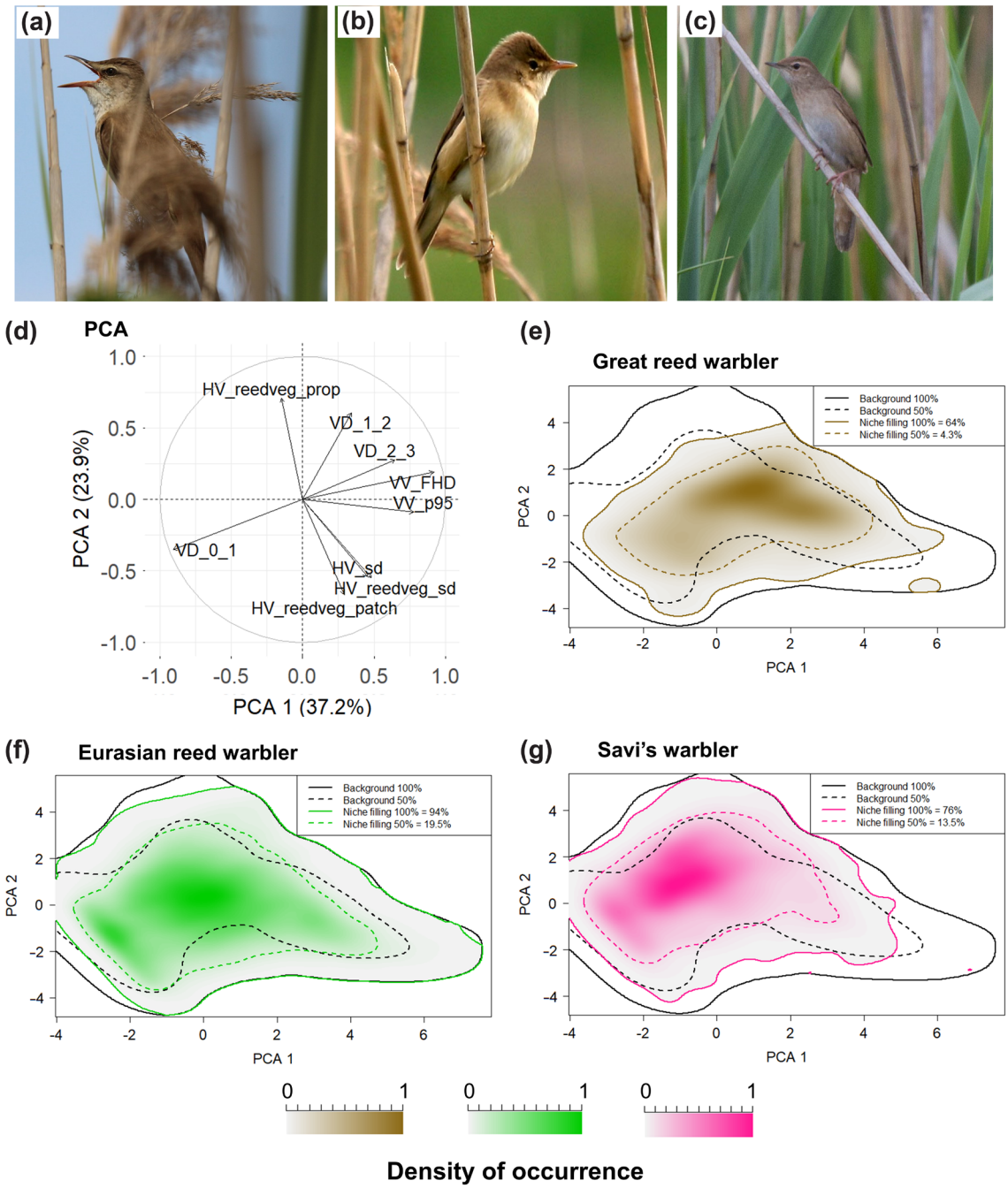

Figure 2. Habitat niches of three reed warbler species in the Netherlands. (a) Great reed warbler *Acrocephalus arundinaceus* (photo credit: Michele Lamberti, source: Flickr). (b) Eurasian reed warbler *Acrocephalus scirpaceus* (photo credit: Martien Brand, source: Wikipedia). (c) Savi's warbler *Locustella luscinioides* (photo credit: Ron Knight, source: Wikipedia). (d) First two axes of a principal component analysis (PCA) based on nine LiDAR metrics capturing vertical vegetation structure and horizontal heterogeneity of vegetation in Dutch wetlands (see metric abbreviations and definitions in Table 1, and variable loadings in the Supporting information). (e–g) Niche filling of the three reed warbler species illustrated with a 50% and 100% kernel density estimation (dashed lines and straight lines, respectively). Niche filling for each species is shown relative to the available background environment (i.e. presence and absence records intersected with LiDAR metrics within wetland-related land cover types).

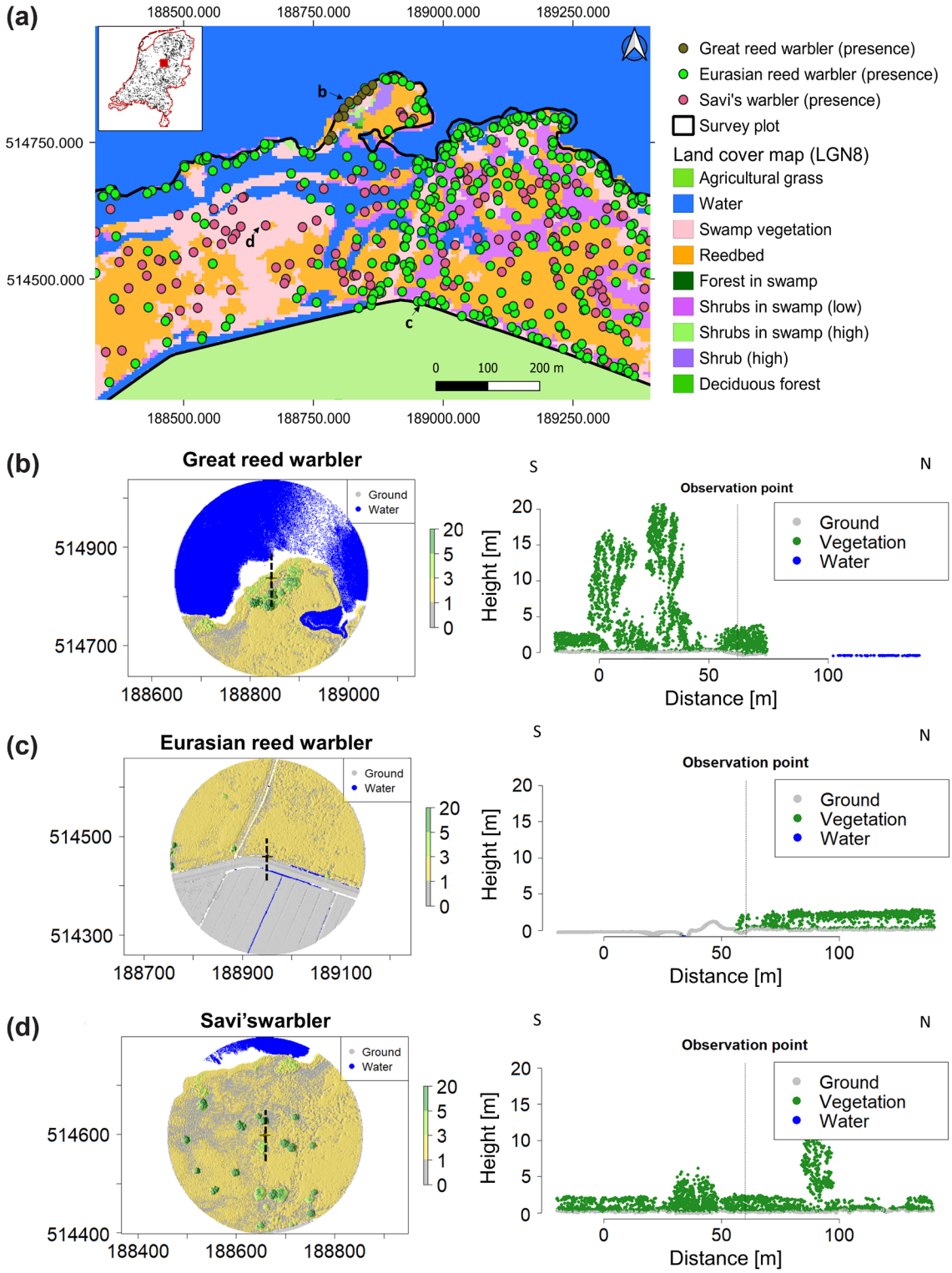

Figure 3. Examples of reed warbler observations in relation to land cover and habitat structure. (a) A typical wetland area near Kampen in the Netherlands in which the Eurasian reed warbler, great reed warbler and Savi's warbler co-occur. The map shows the observed presence observations of all three species (based on territory mapping) in relation to a land cover map (LGN8 at 5 m resolution). (b–d) A typical territory for each of the three species in relation to habitat structure as captured by LiDAR. Left shows a 200 m radius around bird observation points with rasterized 1 m resolution LiDAR data showing the normalized height (z-value) above ground. The colour indicates vegetation classified into height classes (0–1 m: predominantly herbaceous vegetation; 1–3 m: predominantly reed vegetation; 3–5 m: predominantly bushes and small trees and tall reeds; 5–20 m: trees). Right shows a 100 m crossplot (indicated in the left with a dashed line) with the LiDAR point cloud classified into ground, vegetation and water.

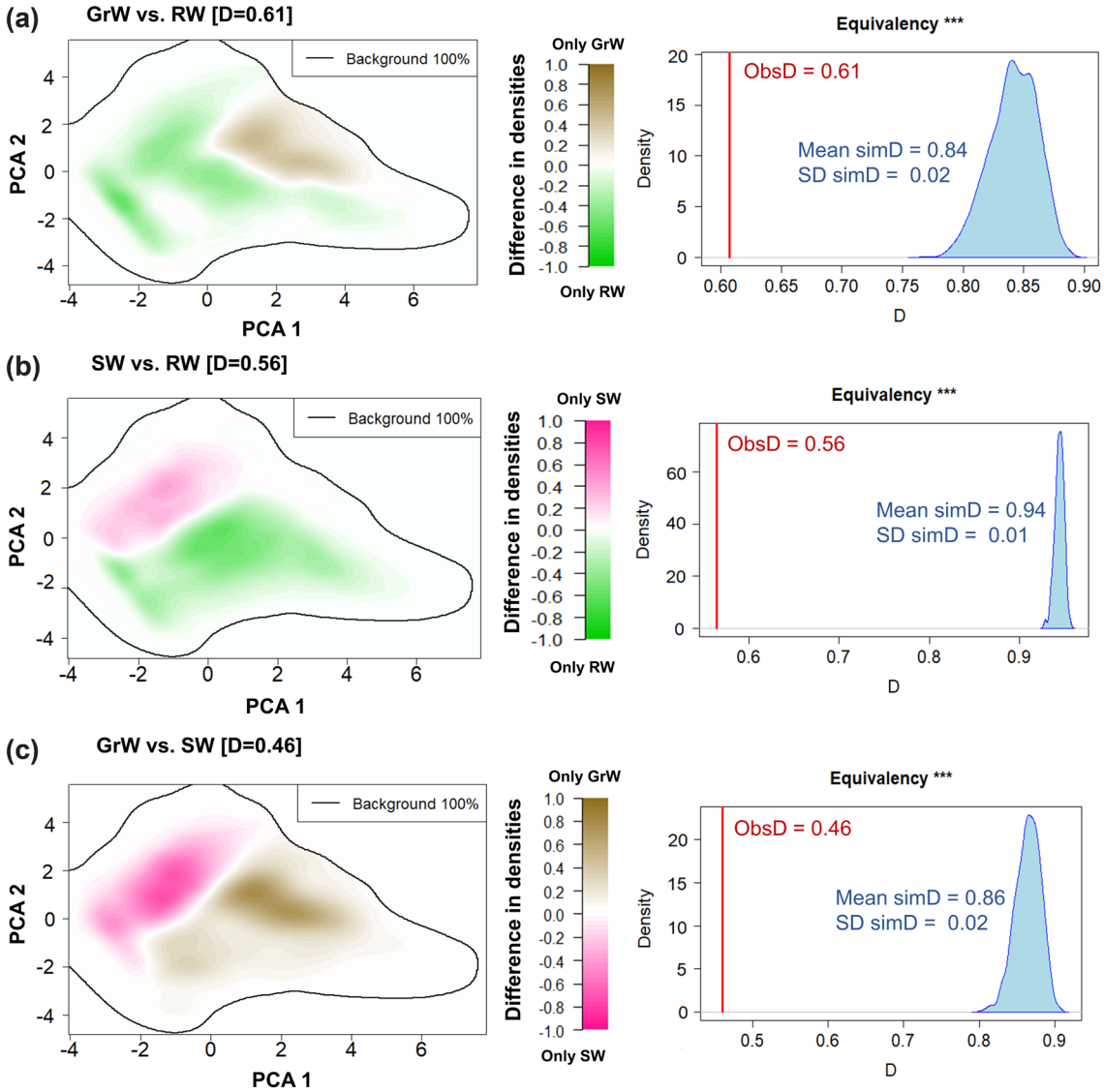

Figure 4. Pair-wise habitat niche comparisons among three reed warbler species (GrW = great reed warbler, RW = Eurasian reed warbler, SW = Savi's warbler). Left: the difference in density of occurrence among two species along two axes of a principal component analysis (PCA 1 and PCA 2, compare Fig. 2d). The outer line indicates the 100% kernel density of the background environment (based on presence–absence records intersected with LiDAR metrics within wetland-related land cover types). Right: results of the niche equivalency test which compares the observed Schoener's D (statistic of niche overlap) with a null distribution of simulated D values based on randomizing the occurrences of both species across their occurrence density grids. ObsD = observed Schoener's D; mean simD = mean of the simulated Schoener's D values; sd simD = standard deviation of the simulated Schoener's D values.

density of low vegetation) and horizontal vegetation structure (extent, patchiness and height variability of reedbeds, and presence of shrubs, trees or water). Our study therefore demonstrates that LiDAR data from country-wide ALS surveys offer promising opportunities for studying niche overlap and niche separation of animals, at unprecedented detail over broad spatial extents. This extends the toolset of ecologists beyond the inclusion of 2D habitat information from land cover maps, not only in forests but also in low-stature ecosystems such as wetlands.

The niche filling analysis revealed that the abundant and widely distributed Eurasian reed warbler occupies a large part (93%) of the available wetland habitat space whereas the two less abundant species (great reed warbler and Savi's warbler) showed considerably less niche filling (69% and 74%). Earlier field studies on niche breadths of reed warblers (marsh warbler, Eurasian reed warbler, great reed warbler, sedge warbler and Savi's warbler) suggest that the great reed warbler and the Savi's warbler are the most specialized species (Rolando and Palestrini 1989). Our study confirms these findings at a national scale using vertical and horizontal vegetation variability metrics derived from LiDAR.

Local field studies suggest that the habitat requirements of the Eurasian reed warbler and the great reed warbler

Table 2. Results of the niche similarity and niche equivalency tests along two axes of a principal component analysis (PCA 1 and PCA 2, compare Fig. 2d). The species column indicates which species are compared (a and b). Observed niche overlap is represented with Schoener's D. The niche equivalency test indicates whether the observed D is statistically different from simulated D values (simD) based on randomly placing occurrences within the density grids of both species. The niche similarity test indicates whether the observed D is statistically more similar than simD based on randomly shifting the occurrence density grids of one species (either a or b) into the background (wetland) environment. We here chose a cell size of 500 × 500 for the occurrence density grids, but results were similar when choosing 100 × 100 and 1000 × 1000 grids (Supporting information). * $p < 0.05$; ** $p < 0.01$; *** $p < 0.001$; ns = not significant.

Species				Niche similarity	
a	b	Niche overlap (D)	Niche equivalency	a→b	b→a
Great reed warbler	Eurasian reed warbler	0.61	different***	similar*	similar*
			mean simD = 0.84	mean simD = 0.29	mean simD = 0.27
			sd simD = 0.02	sd simD = 0.15	sd simD = 0.14
Savi's warbler	Eurasian reed warbler	0.56	different***	ns	similar*
			mean simD = 0.94	mean simD = 0.31	mean simD = 0.23
			sd simD = 0.01	sd simD = 0.15	sd simD = 0.16
Great reed warbler	Savis's warbler	0.46	different***	ns	ns
			mean simD = 0.86	mean simD = 0.19	mean simD = 0.29
			sd simD = 0.02	sd simD = 0.17	sd simD = 0.17

considerably overlap (Graveland 1998, Leisler and Schulze-Hagen 2011). Our niche similarity tests confirm this by showing that their breeding habitat niches are similar. However, our niche equivalency test further revealed that the breeding habitat niches of the two species are separated, i.e. their occurrence densities differ within the available habitat space. Previous field studies report that the great reed warbler prefers structurally diverse and tall reedbeds with some trees and bushes near open water bodies whereas the Eurasian reed warbler is particularly abundant in small patches of reed (Dyrcz 1981, Graveland 1998). Our results confirm this by showing that the great reed warbler is mainly found in vertically complex reed vegetation (PCA 1). Furthermore, our results suggest that both species could occupy similar habitat structures, but that they separate their niches within reedbeds, maybe as a consequence of competition because great reed warblers do not tolerate Eurasian reed warblers in their territories (Leisler and Schulze-Hagen 2011).

The niche similarity tests further revealed that the breeding habitat niche of the Savi's warbler is distinctly different from that of the Eurasian reed warbler, but that the Eurasian reed warblers' breeding habitat niche largely overlapped with the Savi's warbler. Field observations suggest that the Savi's warbler prefers wetland vegetation with a moderate height and a dense ground layer (van der Hut 1985), and large reedbeds mixed with herbaceous fen vegetation (Neto 2006). This is reflected in PCA 2 for which the Savi's warbler showed a higher occurrence density in areas with large and homogenous reedbeds compared to the Eurasian reed warbler. The LiDAR metric 'HH_reedveg_prop' (representing PCA 2) was calculated as the proportion of 10 m grid cells with a vegetation height between 1 and 3 m in a 200 m radius. Besides reed *Phragmites australis*, this vegetation may also include other perennial plants > 1 m such as sedges (*Schoenoplectus*, *Juncus*, *Cladium*) or the bulrush (*Typha*). These are typically dry reed habitats in which the Eurasian reed warbler is rarely found. Instead, the Eurasian reed warbler prefers taller reed vegetation and a low density of vegetation at the ground level (van der Hut 1985). Both aspects were reflected in PCA 1 along which the occurrence densities of the Eurasian reed warbler were higher than those of the Savi's warbler.

The great reed warbler and Savi's warbler were the only species pair for which the niche similarity tests were not statistically significant in both directions, suggesting little competition for the same type of habitat. Territory observations from Hungary suggest that the great reed warbler prefers areas close to open water (e.g. 5 m away from the water edge) whereas the Savi's warbler avoids such habitats (Báldi and Kisbenedek 1999). Moreover, the Savi's warbler prefers large reedbeds and helophyte vegetation with few bushes and trees, a habitat that the great reed warbler would rarely occupy (Báldi 2006). This difference in habitat choice is also reflected along the PCA 2 axis of our analysis which captures the proportion of reed and helophyt vegetation ('HH_reedveg_prop'). Our results therefore suggest a strong niche separation between those two species, probably not driven by competition but by different habitat preferences.

Our analyses support an important role of LiDAR for studying ecological niches at broad spatial scale and with high resolution, especially the aspects of the Grinnellian niche (Grinnell 1917, Soberón 2007). While local in-situ vegetation or habitat studies often measure plant species composition (van der Hut 1985, Neto 2006), LiDAR technology enables the direct measurement of the 3D structure of vegetation, both vertically and horizontally. Field studies can also directly measure vegetation structure in wetlands (e.g. reed stem thickness, ratio between old and new shoots, vegetation cover, maximum height, density of vegetation in height layers or litter thickness) (Dyrcz 1981, van der Hut 1985, Graveland 1998, Neto 2006, Leisler and Schulze-Hagen 2011), but such measurements are costly and time consuming and usually only taken locally (e.g. within a few plots). In contrast, remote sensing data from LiDAR can scale-up to a national level and provide vegetation structural parameters in a standardized way, at high resolution (e.g. 10 m), spatially contiguous and with comparably low costs. Nevertheless, available country-wide ALS datasets also show limitations, e.g. they are often surveyed in winter when broadleaf trees

have no leaves because the main purpose of many LiDAR surveys is terrain mapping (Reutebuch et al. 2005). ALS data captured in winter months may thus not fully represent the variability of vegetation structure within wetlands (Onojeghuo et al. 2010). Future studies should investigate the effect of seasonality of ALS data on capturing vegetation structure within wetlands. Moreover, extending our analyses to other country-wide ALS data would allow us to test whether breeding habitat niches of bird species vary across latitudinal or longitudinal gradients in Europe.

Conclusion

Our study shows that broad-scale analyses of ecological niches can be extended beyond climate, land cover and topography by making use of country-wide ALS datasets to characterize the 3D structure of animal habitats. Combining LiDAR metrics of vegetation structure derived from ALS with niche equivalency and similarity tests thus provides a promising framework for studying fine-scale habitat niches of species over broad spatial extents. The increasing availability of open-access country-wide ALS data therefore opens up new avenues for measuring, monitoring and predicting important aspects of the ecological niche, at an unprecedented resolution and spatial coverage, and even in ecosystems that are predominantly characterized by low-stature vegetation. Future macroecological niche studies should quantify not only aspects of the climate niche, but also integrate fine-scale information on vertical and horizontal vegetation structure derived from LiDAR. With the increasing availability of open-access country-wide ALS data, studies on the geographic variability of fine-scale habitat preferences along latitudinal and longitudinal gradients will also become possible.

Data availability statement

The processed LiDAR data are available from Zenodo (<doi: 10.5281/zenodo.4568243>).

Acknowledgements – We would like to thank the eScience engineers from the Netherlands eScience Center who developed the 'Laserchicken' and 'Laserfarm' software packages: Ou Ku, Yifat Dzigan, Nicolas Renaud, Gijs van den Oord, Bouwe Andela, Faruk Diblen, Elena Ranguelova, Laurens Bogaardt and Romulo Goncalves. Furthermore, we thank the Sovon Dutch Centre for Field Ornithology for providing the bird territory mapping data.
Funding – This work is part of the project 'eScience infrastructure for Ecological applications of lidar point clouds' (eEcoLiDAR) (Kissling et al. 2017), funded by the Netherlands eScience Center (<www.esciencecenter.nl>), grant number ASDI.2016.014.
Author contributions – ZK and WDK conceived the ideas; MWG, CWM and FN pre-processed the LiDAR data with conceptual input from ZK and WDK; ZK designed the analysis of the datasets and interpreted the results with input from WDK, HS and RF; ZK wrote the first draft, WDK substantially improved the initial draft and helped writing the revision of the manuscript. All authors provided ideas, comments and input for the final version.

References

Araújo, M. B. et al. 2019. Standards for distribution models in biodiversity assessments. – Sci. Adv. 5: eaat4858.
Bakx, T. R. M. et al. 2019. Use and categorization of light detection and ranging vegetation metrics in avian diversity and species distribution research. – Divers. Distrib. 25: 1045–1059.
Báldi, A. 2006. Factors influencing occurrence of passerines in the reed archipelago of Lake Velence (Hungary). – Acta Ornithol. 41: 1–6.
Báldi, A. and Kisbenedek, T. 1999. Species-specific distribution of reed-nesting passerine birds across reed-bed edges: effects of spatial scale and edge type. – Acta Zool. Acad. Sci. Hung. 45: 97–114.
Broennimann, O. et al. 2012. Measuring ecological niche overlap from occurrence and spatial environmental data. – Global Ecol. Biogeogr. 21: 481–497.
Brown, J. L. and Carnaval, A. C. 2019. A tale of two niches: methods, concepts and evolution. – Front. Biogeogr. 11: 4.
Chase, J. M. and Leibold, M. A. 2003. Ecological niches: linking classical and contemporary approaches. – Univ. of Chicago Press.
Corti Meneses, N. et al. 2017. Evaluation of green-LiDAR data for mapping extent, density and height of aquatic reed beds at Lake Chiemsee, Bavaria–Germany. – Remote Sens. 9: 1308.
Davies, A. B. and Asner, G. P. 2014. Advances in animal ecology from 3D-LiDAR ecosystem mapping. – Trends Ecol. Evol. 29: 681–691.
Di Cola, V. et al. 2017. ecospat: an R package to support spatial analyses and modeling of species niches and distributions. – Ecography 40: 774–787.
Dyrcz, A. 1981. Breeding ecology of great reed warbler *Acrocephalus arundinaceus* and reed warbler *Acrocephalus scirpaceus* at fishponds in SW Poland and lakes in NW Switzerland. – ACTA Ornithol. 18: 307–334.
Gilbert, G. and Smith, K. W. 2012. Bird–habitat relationships in reedswamps and fens. – Cambridge Univ. Press.
Graveland, J. 1998. Reed die-back, water level management and the decline of the great reed warbler *Acrocephalus arundinaceus* in the Netherlands. – Ardea 86: 187–201.
Grinnell, J. 1917. The niche-relationships of the California thrasher. – Auk 34: 427–433.
Guisan, A. and Thuiller, W. 2005. Predicting species distribution: offering more than simple habitat models. – Ecol. Lett. 8: 993–1009.
Hill, R. A. et al. 2014. Assessing habitats and organism–habitat relationships by airborne laser scanning. – In: Maltamo, M. et al. (eds), Forestry applications of airborne laser scanning: concepts and case studies. Managing forest ecosystems. Springer, pp. 335–356.
Hladik, C. and Alber, M. 2012. Accuracy assessment and correction of a LIDAR-derived salt marsh digital elevation model. – Remote Sens. Environ. 121: 224–235.
Holt, R. D. 2009. Bringing the Hutchinsonian niche into the 21st century: ecological and evolutionary perspectives. – Proc. Natl Acad. Sci. USA 106: 19659–19665.
Hopkinson, C. et al. 2005. Vegetation class dependent errors in lidar ground elevation and canopy height estimates in a boreal wetland environment. – Can. J. Remote Sens. 31: 191–206.

Hutchinson, G. E. 1957. Population studies – animal ecology and demography – concluding remarks. – Cold Spring Harbor Symp. Quant. Biol. 22: 415–427.
Kerr, J. T. and Ostrovsky, M. 2003. From space to species: ecological applications for remote sensing. – Trends Ecol. Evol. 18: 299–305.
Kissling, W. D. et al. 2017. eEcoLiDAR, eScience infrastructure for ecological applications of LiDAR point clouds: reconstructing the 3D ecosystem structure for animals at regional to continental scales. – Res. Ideas Outcomes 3: e14939.
Koma, Z. et al. 2020. Classifying wetland-related land cover types and habitats using fine-scale lidar metrics derived from country-wide airborne laser scanning. – Remote Sens. Ecol. Conserv. doi: 10.1002/rse2.170.
Lefsky, M. A. et al. 2002. Lidar remote sensing for ecosystem studies. – BioScience 52: 19–30.
Leisler, B. and Schulze-Hagen, K. 2011. The reed warblers: diversity in a uniform bird family. – KNNV Publishing.
Lucas, C. et al. 2019. Identification of linear vegetation elements in a rural landscape using LiDAR point clouds. – Remote Sens. 11: 292.
Luo, S. et al. 2015. Estimation of wetland vegetation height and leaf area index using airborne laser scanning data. – Ecol. Indic. 48: 550–559.
Luo, S. et al. 2017. Retrieving aboveground biomass of wetland *Phragmites australis* (common reed) using a combination of airborne discrete-return LiDAR and hyperspectral data. – Int. J. Appl. Earth Observ. Geoinform. 58: 107–117.
Meijer, C. et al. 2020. Laserchicken – a tool for distributed feature calculation from massive LiDAR point cloud datasets. – SoftwareX 12: 100626.
Neto, J. M. 2006. Nest-site selection and predation in Savi's warblers *Locustella luscinioides*. – Bird Study 53: 171–176.
Nie, S. et al. 2018. Estimating the height of wetland vegetation using airborne discrete-return LiDAR data. – Optik 154: 267–274.
Onojeghuo, A. O. et al. 2010. Characterising reedbed habitat quality using leaf-off LiDAR data. – 2010 6th Int. Colloq. Signal Process. Its Appl. doi: 10.1109/CSPA.2010.5545322.
Pearman, P. B. et al. 2008. Niche dynamics in space and time. – Trends Ecol. Evol. 23: 149–158.
Petitpierre, B. et al. 2012. Climatic niche shifts are rare among terrestrial plant invaders. – Science 335: 1344–1348.
Pettorelli, N. et al. 2016. Framing the concept of satellite remote sensing essential biodiversity variables: challenges and future directions. – Remote Sens. Ecol. Conserv. 2: 122–131.
Reutebuch, S. E. et al. 2005. Light detection and ranging (LIDAR): an emerging tool for multiple resource inventory. – J. For. 103: 286–292.
Rolando, A. and Palestrini, C. 1989. Habitat selection and interspecific territoriality in sympatric warblers at two italian marshland areas. – Ethol. Ecol. Evol. 1: 169–183.
Schurr, F. M. et al. 2012. How to understand species' niches and range dynamics: a demographic research agenda for biogeography. – J. Biogeogr. 39: 2146–2162.
Soberón, J. 2007. Grinnellian and Eltonian niches and geographic distributions of species. – Ecol. Lett. 10: 1115–1123.
Soberón, J. and Nakamura, M. 2009. Niches and distributional areas: concepts, methods and assumptions. – Proc. Natl Acad. Sci. USA 106: 19644–19650.
van der Hut, R. M. G. 1985. Habitat choice and temporal differentiation in reed passerines of a Dutch marsh. – Ardea 74: 159–176.
Vergeer, J.-W. et al. 2016. Handleiding Sovon Broedvogelonderzoek: Broedvogel Monitoring Project en Kolonievogels. – Sovon Vogelonderzoek Nederland, Nijmegen.
Vierling, K. T., et al. 2008. Lidar: shedding new light on habitat characterization and modeling. –Front. Ecol. Environ. 6: 90–98.
Warren, D. L. et al. 2008. Environmental niche equivalency versus conservatism: quantitative approaches to niche evolution. – Evolution 62: 2868–2883.
Zellweger, F. et al. 2013. Remotely sensed forest structural complexity predicts multi species occurrence at the landscape scale. – For. Ecol. Manage. 307: 303–312.
Zellweger, F. et al. 2014. Improved methods for measuring forest landscape structure: LiDAR complements field-based habitat assessment. – Biodivers. Conserv. 23: 289–307.